Spatial and Temporal Oscillation at Si(111) Electrodes in Aqueous Fluoride-Containing Solution

H. J. Lewerenz

Department of Interfaces, Bereich Physikalische Chemie, Hahn-Meitner-Institut Berlin, Glienicker Strasse 100, D-14109 Berlin, Germany

Received: August 30, 1996; In Final Form: February 2, 1997[⊗]

The oscillatory behavior of single crystalline n-Si(111) in dilute ammonium and sodium fluoride solutions is investigated. Simultaneous in-situ Fourier transform infrared analyses performed in the multiple internal reflection (FTIR-MIR) mode and photocurrent measurements show a pronounced variation in the integrated Si−O signal during photocurrent oscillations and corresponding changes in minority excess carrier concentration. The resulting oxide thickness changes are ±5 monolayers (ML), assuming an average thickness value of 22 ML (as a lower limit due to the inaccessibility of Si−F vibrations in the FTIR experiment). The investigation of the initial oxidation by light-generated holes shows the formation of oxide in two stages. Electrolytic coupling of the oscillations is demonstrated in experiments in which oscillations of electrodes with spatially separated areas on their surfaces are studied.

Introduction

Oscillatory phenomena are observed in many physical, chemical, and biological systems.[1−6] Particularly interesting features occur, for instance, in catalytic reactions[7−9] and in several biological entities (structures).[10−12] The phenomenon has also long been well-known in the electrochemistry of metals[13−15] and, more recently, of semiconductors.[16−23] The common underlying concept of these widespread phenomena involves nonlinear terms in the kinetic equations of open systems far from equilibrium, observable, for instance, in positive and negative feedback loops. In chemical systems, the autocatalytical step is an example of coupling by a positive feedback. Whereas the mechanisms responsible for the oscillations have been identified for most of the a.m. systems, a similarly detailed understanding of the current oscillations at Si electrodes immersed in fluoride-containing electrolytes has not yet been achieved.

This is in part due to the fact that the investigations concerning the oscillating behavior of Si electrodes are rather recent, and since the oscillations involve a comparably large set of experimental parameters, little is known about the physicochemical origin of the oscillatory behavior. In particular, it is the three dimensionality involving a growing and dissolving oxide layer, three interfaces (silicon−oxide, silicon−electrolyte, silicon oxide−electrolyte), transport of charge through these interfaces and films, and possible electrolytic coupling as suggested by Chazalviel and Peter.[24] This latter topic will be in part addressed in the present article (see below).

Being of purely fundamental interest at first, it has turned out that photocurrent oscillations can be used to produce, in a two-step procedure, high-quality H-terminated Si(111) surfaces.[25−28] Such surfaces exhibit an interface state density of about 10^{10} cm^{-2} eV^{-1},[27,28] and they are smoother than surfaces obtained by electropolishing.[29,30] This technological result has in turn stimulated further research concerning the detailed understanding of the phenomenon.[31−33] The present model is based on the postulation of pores of about 100 nm width which change in radii and number during the current oscillation.[23] Such pores have indeed been observed,[32] and their existence explains the high modulation depth of the (photo)currents during oscillations although an oxide layer of substantial thickness is present on the surface. The mechanism of coupling of the pores has not yet been elucidated. Electrolytic coupling as well as electronic changes at illuminated samples kept at fixed potential could be considered. The present concept assumes that current flow through pores is mostly responsible for the oscillations.[23,32]

In this article, new detailed in-situ analyses on the interfacial changes at n-Si(111) during photocurrent oscillation will be presented. They will show that the original fluctuating pore model has to be modified. In addition, the initial surface transformation of the electrode prior to oscillations is investigated, and an experiment on the spatial behavior of the oscillations is presented.

Experimental Section

Electrochemical experiments were made in specifically designed plastic cells equipped with Pt counter electrodes and saturated calomel electrodes (SCE) as reference. All solutions were made from highest purity chemicals as available (analytical grade or ultrapure) and triply distilled water. Experiments were made using the standard three-electrode potentiostatic arrangement with an EG&G 273 potentiostat/galvanostat. For illumination, white light from a 250 W tungsten−iodine lamp was used.

The n-type silicon samples were (111)-oriented without miscut and P-doped. The specific resistivity of the float zone material ranged from 6 Ω cm (electrochemical experiments) to 50 Ω cm (infrared experiments). Back contacts were made by an In−Ga alloy. For encapsulation a silicon epoxy was used.

In-situ infrared measurements were done in an especially designed cell.[29] Because of the high multiphonon absorption losses in Si, the wavenumber region of the asymmetric Si−O stretching mode is difficult to investigate in the standard ATR-MIR (attenuated total reflection−multiple internal reflection) geometry using large crystals. To reduce the optical path length, we use a thin sample of considerably smaller dimensions (area 0.14 cm^2) in order to become more sensitive in the spectral region between 1000 and 1300 cm^{-1}. The optical path length is hence reduced from 70 to 11 mm. The measuring cell has a Pt counter electrode ring and a 0.1 M KCl/Ag/AgCl reference

[⊗] Abstract published in *Advance ACS Abstracts,* March 1, 1997.

S1089-5647(96)02694-6 CCC: $14.00

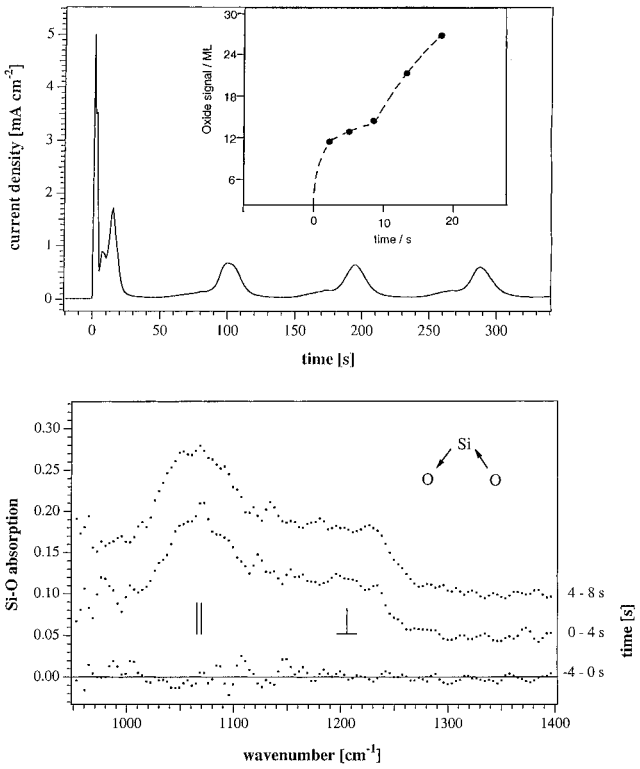

Figure 1. Vibrational analysis of the initial surface changes of Si(111) induced by illumination: (a, top) Photocurrent vs time showing a multiple initial peak structure and the beginning of regular oscillations. Insert: evaluation of the initial Si−O signal by integrating spectra as shown in (b). (b, bottom) FTIR spectra in the region of the asymmetric Si−O stretching mode for three time regimes (see text): 0.1 M NaF, pH 4, $I = 10$ mW cm^{-2}, $V = +6$ V (SCE).

electrode. As potentiostat, a HEKA model was chosen, and eight scans were made per spectrum (0.5 s per scan) in order to be able to follow the rapid changes during the initial stages of photocurrent oscillations. The measurements were performed in a commercial Bruker infrared spectrometer.

Results and Discussion

In a series of articles, we have described various electrochemical methods to produce hydrogen-terminated Si surfaces with high electronic quality.[35−40] The best surfaces with respect to surface morphology[29] and superior electronic quality[26] were obtained in procedures that employed oxidation of the silicon electrode during photocurrent oscillation, emersion of the samples after about 15 cycles, and subsequent oxide removal during and after the flow of a transient dark current. This treatment was also used in the experiments presented here in order to start from comparable conditions and high surface quality. Figure 1 shows the photocurrent vs time for a sample at +6 V (SCE) after switching on the light at $t = 0$ s. The solution parameters are adjusted such that a sustained photocurrent oscillation sets in. It can be seen from Figure 1 that, before the oscillations arise, two well-separated current peaks are observed. These photocurrent peaks reach substantially higher values than the maxima of the following oscillation. Figure 1b shows the infrared absorption due to the asymmetric Si−O stretching mode in the temporal regime of the first current maximum. The parallel as well as the perpendicular component of the Si−O stretching mode is well-resolved at 1060 and 1230 cm^{-1}, respectively. The behavior of the IR signal obtained during and after the second current maximum for 10 s $\leq t \leq$ 25 s is not displayed in Figure 1b as no qualitative changes occur compared to the data displayed between 0 and 8 s.

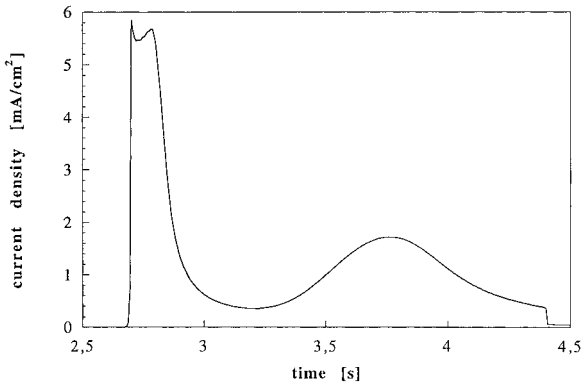

Figure 2. Initial photocurrent peaks prior to oscillatory behavior at higher temporal resolution; 0.1 M NH_4F, pH 3.9, $I = 100$ mW cm^{-2}, $V = +6$ V (SCE).

Instead, the development of the integrated Si−O signal is displayed in the insert of Figure 1a. From comparison between the insert of Figure 1a and the current behavior in this figure, it can be seen that both initial maxima are related to the formation of silicon oxide. In a separate experiment, we have oxidized Si in fluoride-free solution at low current density and measured the charge flux simultaneously with the integrated signal due to Si−O in the wavenumber range from 1000 to 1300 cm^{-1}. Since in this separate experiment, the sample potential was too low for oxygen evolution, we could calibrate the Si−O signal integral with respect to oxide coverage in monolayers. The inset of Figure 1a shows the corresponding evaluation. It is seen that the initial current results in the formation of an approximately 50 Å thick oxide during the first 2 s after illumination. The current minimum at about $t = 5-10$ s is revealed in the insert by a plateau in oxidic coverage, and the second maximum then results in a further increase of the oxide thickness. This increase, however, is not as steep with time as for the first peak. The initial passivation appears not to be complete since the current only drops to about 500 μA cm^{-2}. Presumably, the fast initial oxidation results in an island type of oxide growth whereas the second oxidation leads to almost complete passivation, indicating the formation of two oxide types which are associated with the occurrence of oscillations. Taking the charge contained in these peaks, one obtains approximately 15 and 20 ML for the initial and the second peak, respectively. Comparing these values with the data shown in the inset of Figure 1a indicates that, during the initial peak, the oxide formation efficiency is close to 1 whereas the reduced thickness derived from the Si−O signal of the second peak could mean that oxygen evolution does occur or that fluoride is incorporated into the oxide. Since the passivation is improved after the second peak (see also Figure 2), it appears more likely that charge is lost in the oxygen evolution reaction at an already existing inhomogeneous oxide.

The period of the oscillations can be changed drastically by the solution composition, and a proportionality between oscillation frequency and etch rate has been found.[23] In Figures 2 and 3, the initial current peaks (Figure 2) and photocurrent oscillations with a period of about 50 s are displayed (Figure 3). Figure 3 also shows the change of the integrated Si−O signal relative to the average value. Although the height of the current maxima in Figure 2 is similar to those in Figure 1a, the shorter time scale in the former leads to a thinner oxide under these experimental conditions. This in turn obviously increases the oscillation frequency (higher etch rate, thinner oxide). The average value of 35 for the intergrated oxide signal corresponds to a 22 ML equivalent. The change in the overall Si−O signal corresponds to ±5 ML. Hence, the oxide coverage

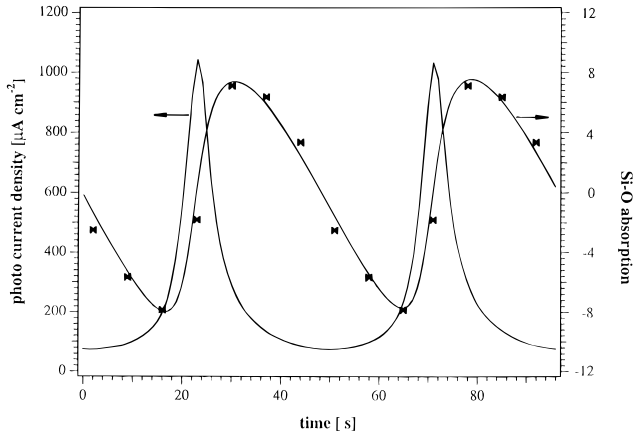

Figure 3. Simultaneous in-situ measurement of photocurrent and integrated Si−O vibrational signal vs time during oscillation (see text); 0.1 M NaF, pH 3.9, $I = 10$ mW cm^{-2}, $V = +6$ V (SCE).

varies between about 17 and 27 ML during the oscillations shown in Figure 3, whereas the oxide signal in Figure 1a reaches 32 ML before the oscillations. Two further interesting features are contained in Figure 3: first, a shift between photocurrent maxima and oxide signal maxima is observed; second, the asymmetry between current maxima and minima is reflected by different slopes for increase and decrease of the Si−O signal. Photocurrent maxima occur at the inflection point of the increasing Si−O signal, the current minima start at maximum integrated oxide signal, and at or slightly before the minimum Si−O signal the photocurrent starts to rise. The different slopes in the Si−O signal indicate different formation and dissolution rates for the oxide. Obviously, the dissolution (or etching) reaction according to

$$SiO_2 + 6HF \rightarrow SiF_6^{2-} + 2H_2O + 2H^+ \quad (1)$$

$$SiO_2 + 3HF_2^- \rightarrow SiF_6^{2-} + 2H_2O + OH^- \quad (2)$$

is slower than the formation reaction, leading to a sustained passivation of the sample as is revealed by the prolonged periods of minimal current. The inflection point of the integrated signal of the Si−O vibration (for instance at $t = 49$ s in Figure 3) coincides with the absolute minimum of $i_{ph}(t)$. It is also interesting to note that obviously the direction of change has an influence on the current. In the decreasing branch of the Si−O signal, for instance at $t = 58$ s, i_{ph} is about 100 μA cm^{-2}. For the same value of Si−O at $t = 21$ s, the current is larger by a factor more than 5.

In-situ ellipsometric as well as ex-situ X-ray photoelectron spectroscopic (XPS) investigations during and after oscillatory cycles have revealed very little changes in the oxide thickness.[31,32,41,42] This is related to the emersion of the samples at the current maxima and minima, and it can be seen from Figure 3 that the oxide signal is then close to the average value. Although a pronounced variation in Δ has been found with ellipsometry, these variations have been explained by variation in the refractive index of the covering oxidic film using an effective medium theory assuming pore changes to be solely responsible for the current variations.[32,43] In view of the new experimental data, this interpretation has to be corrected. The data in Figure 3, former ellipsometry results, and transmission electron micrographs show that changes in pore number and radii as well as overall oxide thickness changes occur during photocurrent oscillations. The changes during the fluctuations of the pores are too small to produce the Si−O changes in Figure 3. Taking pore density and radii from refs 31 and 32 and calculating the pore volume from data on oxide thickness, the absolute expected change in the Si−O signal would be 10%, i.e., about 2 ML, whereas Figure 3 indicates an absolute change of 10 ML, which corresponds to 45%.

Interestingly, a shift similar to the one observed between oxide signal and photocurrent is found upon reinspection of simultaneous photocurrent and in-situ excess microwave reflectivity measurements.[19,44] Whereas for maxima of i_{ph} the microwave signal is minimal, microwave signal maxima occur when the photocurrent begins to rise toward a maximum. This is quite exactly the temporal region, when the Si−O signal is minimal, or the time point at which the oxide dissolution is overcompensated by its formation. These features have been explained by an interplay of surface recombination rate and charge transfer rate.[44] The charge transfer rate k_r starts to increase from a low value due to sustained passivation in the photocurrent minimum, and the surface or interface recombination velocity S_r drops drastically toward the end of the current minimum, indicating that the etch front reaches an oxide interface with improved electronic properties. Since both k_r and S_r are small when the new oxide is beginning to be formed, the microwave signal is at its maximum due to light-induced charge carrier accumulation. The electronic implications which could be envisaged might result in a pronounced positive shift of the silicon band edges. Such a scheme is shown in Figure 4. Initially, in the dark with the very low dark current of hydrogen-terminated samples, the situation can be envisaged as in Figure 4a, with a large potential drop occurring in the sample. Upon illumination the initial oxide is formed (see two peaks and insert of Figure 1), and further charge transfer is inhibited (Figure 4b). The light-induced minority carriers are now accumulated at the silicon surface, resulting in a positive charge of the structure with a corresponding band edge shift while oxide dissolution occurs simultaneously. Further oxidation is additionally inhibited due to a flattening of the bands (Figure 4c). In this situation the oxide dissolution rate dominates over the formation rate, and most of the light-generated excess carriers will recombine. The applied external potential of 6 V, as an example, is kept constant, and a substantial part will in this situation drop at the electrolyte interface. In earlier experiments it has been shown that the silicon oxide etch rate k_e in the fluoridic electrolyte after Judge[45] is proportional to the oscillation frequency,[23] indicating the importance of this step of oxide dissolution at positively shifted band edges. When the outer part of the oxide is thin enough to allow contact through pores, for instance, the situation is reversed, the holes are no longer accumulated, and the band edges shift upward toward more negative potential. The transition from the situation shown in Figure 4c to Figure 4b is shown in Figure 4d. Subsequently, partial oxidation sets in, resulting then in the situation shown in Figure 4b, in which the cycle begins again. This suggestion does not include the role of the electrolyte and the lateral inhomogeneities of the oxide-(pores), but it should be noted that periodic changes in the electric field at the semiconductor/oxide/electrolyte contact can play an important role in further elucidating the underlying mechanism.

The TEM data, in-situ ellipsometry,[32] and the results in Figures 1 and 3 indicate that current flow occurs at defective parts of the oxide, thus supporting the earlier proposed fluctuating pore model:[23] the minimum oxide thickness for the thinner oxide shown in Figure 3 (coverage 17 ML) is too thick to allow efficient charge transfer, assuming a homogeneous thickness. In addition, XPS analyses show a nonnegligible fluoride signal. Since the IR absorption of Si−F is outside the measuring range of the experiment, the measured and integrated Si−O signal

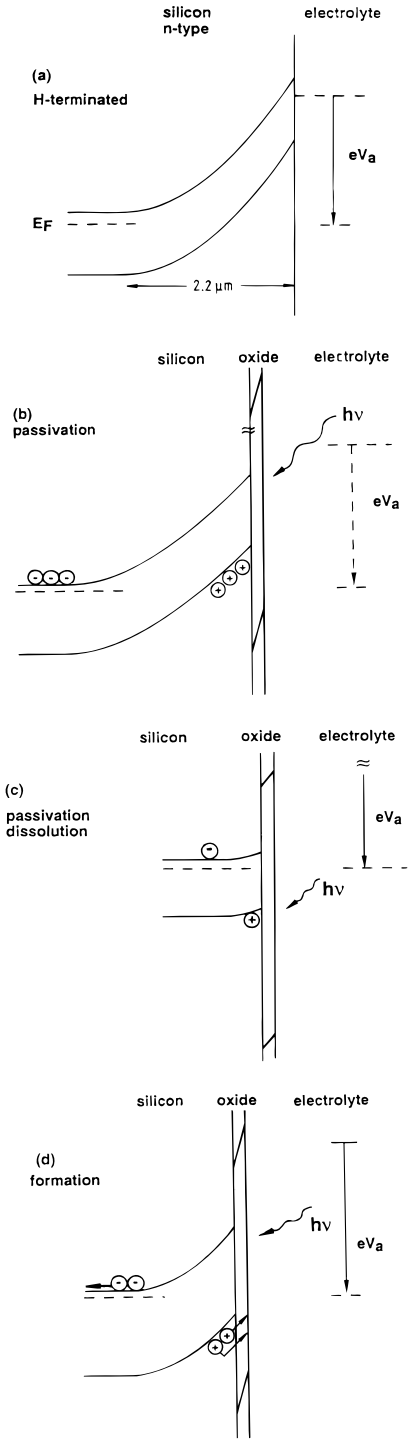

Figure 4. Schematic of the electronic situation at the silicon/electrolyte junction at high anodic potential and low dark current flow: (a) initial situation of the hydrogen-terminated electrode; (b) passivation by corrosion reaction of light-generated holes; (c) band edge shift after passivation and oxide dissolution; (d) reoxidation of the thinnened oxide (see also text).

represents a lower limit for the actual film thickness, due to the missing contribution from Si−F species.

The oscillatory behavior considered above was related to temporal changes and related changes in the passivating film. The observed nonuniformity of this film, evidenced by micropore formation, leads to the problem whether a spatial coupling of the oscillations via processes in the electrolyte can be determined. Therefore, the oscillations of partly and fully immersed electrodes under illumination were monitored. Figure 5 shows two sets of experiments: in Figure 5a, the lower half

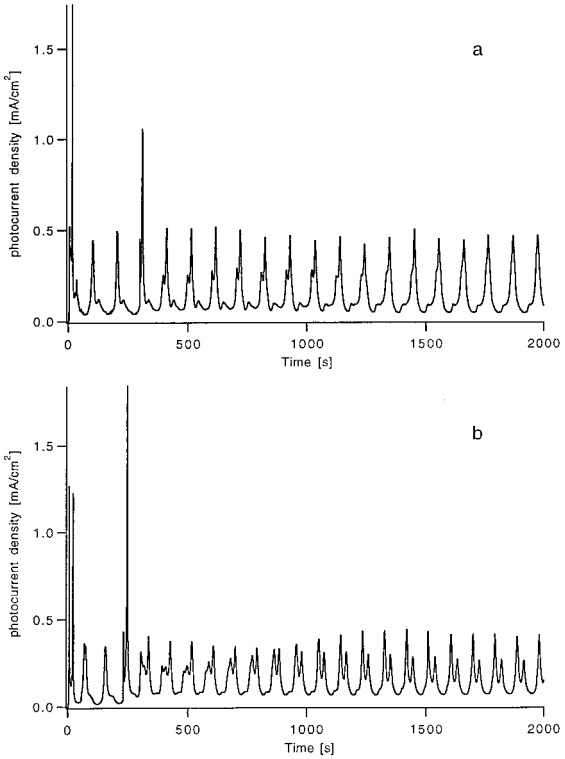

Figure 5. Temporal behavior of photocurrent oscillations for two sets of experiments. (a) Immersion of the upper half of the sample at $t =$ 293 s. (b) Immersion of the upper half at $t = 233$ s. The two areas were separated spatially by an epoxy stripe; 0.1 M NH_4F, pH 4, $i = 27$ mW cm^{-2}, $V = +5.5$ V (SCE).

of an electrode was immersed into ammonium fluoride solution, and at $t = 0$ the light was switched on. After the well-known double-peak structure the photocurrent oscillations set in after 103 s. Shortly before the third oscillation, the upper part of the electrode was immersed and illuminated ($t = 293$ s). The double-peak structure sets in at $t = 293$ s; the second maximum at $t = 304$ s overlaps with the earlier started oscillation of the lower sample part. The coexistence of two photocurrent peaks is observed during the next 10 oscillations ($f = 9.57 \times 10^{-3}$ Hz, $T = 104.5$ s). At $t = 1500$ s, the smaller photocurrent signal ($\Delta t \approx 16$ s) begins to cede, and a single oscillation with the phase of the first oscillation remains. It should be noted that the frequency (or period) decreases (increases) very slightly with time. After 6000 s, it changed from $f = 9.57 \times 10^{-3}$ Hz (104.5 s) to $f = 8.96 \times 10^{-3}$ Hz (111.6 s). The experiment shown in Figure 5a shows the behavior of an oscillating Si electrode, and the disapperance of the second oscillation indicates an interaction between the oscillating sites. This coupling, however, could also arise from the applied electric field (6 V anodic potential). In order to distinguish between semiconductor and electrolytic effects, a very similar experiment to the one shown in Figure 5a was performed. The only difference was that in the second experiment the surface of the electrode was separated by a stripe of epoxy of about 3.5 mm width.

The resulting behavior is shown in Figure 5b. There, the upper part is immersed under illumination at $t = 233$ s. Here, too, the second oxide formation peak coincides with the initial oscillation of the lower part. The two resulting oscillations of the photocurrent remain separated. Even for $t > 6000$ s (not shown here), no change in the fundamental oscillatory behavior is found.[46] The result of Figure 5 shows that electrolytic coupling is important at the Si/passive film/ammonium fluoride junction. It might be envisaged that lateral interactions originate

from very local current transport effects through the oxidic film. The anodic charge transferred at micropores and similar defective sites has to be counteracted by the movement of anions to restore charge neutrality. This process involves diffusion (medium- to long-range interaction) and drift (short-range) in the region around pores where the electric field is changed by charge transfer. Migration effects due to inhomogeneous Helmholtz layers at the oxide−electrolyte interface as observed on metals[47] cannot be excluded here, since the electric field in the Helmholtz layer can be large enough even if most of the applied potential drop occurs in the oxide and the semiconductor space charge although it will be much smaller compared to the situation at metal−electrolyte interfaces. As shown in Figure 4, the contribution from the electric field within the semiconductor could dominate the behavior. At present, it appears clear that two types of oxidic films are formed.[48] The existence of electrolytic coupling of the photocurrent oscillations has also been found in experiments in which sodium and potassium salts are added to the ammonium fluoride solution, resulting in a pronounced change of the oscillation period.[49]

In the intent to elucidate the physicochemical changes of the silicon/passive film/fluoridic electrolyte structure associated with oscillating currents, a substantial change in oxide thickness, the initial formation of two types of oxides, and a spatial coupling via the electrolyte have been found. It still appears that the current transport takes place at micropores since the minimum integrated oxide signal is too large for charge transfer if a homogeneous passive film thickness is assumed. Despite the increased information on the microscopic changes of the structure, the information for a mathematical formulation of the problem does not yet suffice. It is in particular the identification and assignment of the physical and chemical factors which enter the corresponding differential equation which is problematic. The suggestion based on electronic changes shown in Figure 4 can only in part explain the behavior as it does include neither the lateral electrolytic coupling nor the influence of pores. Nevertheless, the application of advanced in-situ and ex-situ vibrational analysis, optical and electron spectroscopy, transmission electron microscopy, and scanning probe microscopy makes this author optimistic that the basic contributing factors can be eventually identified.

Acknowledgment. The author is indebted to Dr. Jörg Rappich and Stefan Rauscher for their contribution to the infrared measurements and many enlightening discussions, to Jesco Möller for a series of experiments on electrolytic coupling, and to Drs. Helmut Jungblut and Jürgen Crzanna for critical reading of the manuscript.

References and Notes

(1) Prigogine, I. *Introduction to Thermodynamics of Irreversible Processes*; Wiley: New York, 1961.
(2) Field, R. J., Burger, M., Eds. *Oscillations and Travelling Waves in Chemical Systems*; Wiley: New York, 1985.
(3) Zhabotinsky, A. M. *Chaos* **1991**, *1*, 379.
(4) Ross, J.; Schell, M. *Annu. Rev. Biophys. Chem.* **1987**, *16*, 401.
(5) Tributsch, H.; Bogomolni, R. A. *Chem. Phys. Lett.* **1994**, *227*, 74.
(6) Haken, H. *Synergetics. An Introduction*; Springer-Verlag: Heidelberg, 1977.
(7) Ertl, G. *Adv. Catal.* **1990**, *40*, 213.
(8) Keil, W.; Wicke, E. *Ber. Bunsen-Ges. Phys. Chem.* **1980**, *84*, 377.
(9) Rotermund, H. H.; Engel, W.; Kordesch, M.; Ertl, G. *Nature* **1990**, *343*, 355.
(10) Prigogine, I. *Self Organization in Non-Equilibrium Systems*; Wiley: New York, 1977.
(11) Meinhardt, H.; Klingler, M. *J. Theor. Biol.* **1987**, *126*, 63.
(12) Beeler, G. W.; Reuter, H. *J. Physiol.* **1977**, *268*, 177.
(13) Hudson, J. L.; Bassett, M. R. *Rev. Chem. Eng.* **1991**, *7*, 109.
(14) Franck, U. F.; Hugh, R. Fitz *Z. Elektrochem.* **1961**, *65*, 156.
(15) Flätgen, G.; Krischer, K. *Phys. Rev.* **1995**, *E51*, 3997.
(16) Stumper, J.; Greef, R.; Peter, L. M. *J. Electroanal. Chem.* **1991**, *310*, 445.
(17) Gerischer, H.; Lübke, M. *Ber. Bunsen-Ges. Phys. Chem.* **1988**, *92*, 573.
(18) Chazalviel, J. N.; Etman, A.; Ozanam, F. *J. Electroanal. Chem.* **1991**, *297*, 533.
(19) Lewerenz, H. J.; Schlichthörl, G. *J. Electroanal. Chem.* **1992**, *327*, 85.
(20) Föll, H. *Appl. Phys.* **1991**, *A53*, 8.
(21) Turner, D. R. *J. Electrochem. Soc.* **1958**, *105*, 402.
(22) Lehmann, V.; Föll, H. *J. Electrochem. Soc.* **1990**, *137*, 653.
(23) Lewerenz, H. J.; Aggour, M. *J. Electroanal. Chem.* **1993**, *8*, 2548.
(24) Chazalviel, J. N.; Peter, L. M. *J. Electroanal. Chem.* **1962**, *327*, 343.
(25) Dittrich, Th.; Angermann, H.; Flietner, H.; Bitzer, Th.; Lewerenz, H. J. *J. Electrochem. Soc.* **1994**, *141*, 3597.
(26) Dittrich, Th.; Rauscher, S.; Bitzer, Th.; Aggour, M.; Flietner, H.; Lewerenz, H. J. *J. Electrochem. Soc.* **1995**, *142*, 2411.
(27) Rauscher, S.; Dittrich, Th.; Aggour, M.; Rappich, J.; Flietner, H.; Lewerenz, H. J. *Appl. Phys. Lett.* **1995**, *66*, 3018.
(28) Ennaoui, A.; Aggour, M.; Lilie, J.; Lewerenz, H. J. Submitted for publication.
(29) Rappich, J.; Lewerenz, H. J. *Electrochim. Acta* **1996**, *41*, 675.
(30) Rappich, J.; Jungblut, H.; Aggour, M.; Lewerenz, H. J. *J. Electrochem. Soc.* **1994**, *141*, L99.
(31) Aggour, M. Ph.D. Thesis, Technical University Berlin, 1994.
(32) Aggour, M.; Giersig, M.; Lewerenz, H. J. *J. Electroanal. Chem.* **1995**, *383*, 67.
(33) Rappich, J.; Lewerenz, H. J.; Gerischer, H. *J. Electrochem. Soc.* **1993**, *140*, L187.
(34) Ozanam, F.; Da Fonseca, C.; Chazalviel, J. N. *Proc. Indian Acad. Sci. Chem. Sci.* **1995**, *107* (6), 709.
(35) Bitzer, T.; Lewerenz, H. J. *Surf. Sci.* **1992**, *269/270*, 886.
(36) Lewerenz, H. J.; Bitzer, T. *J. Electrochem. Soc.* **1992**, *139*, L21.
(37) Lewerenz, H. J.; Bitzer, T.; Gruyters, M.; Jacobi, K. *J. Electrochem. Soc.* **1993**, *140*, L44.
(38) Bitzer, T.; Lewerenz, H. J.; Gruyters, M.; Jacobi, K. *J. Electroanal. Chem.* **1993**, *359*, 287.
(39) Bitzer, T.; Gruyters, M.; Lewerenz, H. J.; Jacobi, K. *Appl. Phys. Lett.* **1993**, *63*, 397.
(40) Jacobi, K.; Gruyters, M.; Geng, P.; Bitzer, T.; Aggour, M.; Rauscher, S.; Lewerenz, H. J. *Phys. Rev.* **1995**, *B51*, 5437.
(41) Bitzer, T. Ph.D. Thesis, Technical University Berlin, 1992.
(42) Stumper, J.; Greef, R.; Peter, L. M. *J. Electroanal. Chem.* **1991**, *310*, 445.
(43) Bruggeman, D. A. G. *Ann. Phys.* **1935**, *5*, 636.
(44) Lewerenz, H. J.; Schlichthörl, G. *J. Appl. Phys.* **1994**, *75*, 3544.
(45) Judge, J. S. *J. Electrochem. Soc.* **1971**, *118*, 1772.
(46) Möller, J.; Lewerenz, H. J. To be published.
(47) Flätgen, G.; Krischer, K. *J. Chem. Phys.* **1995**, *103*, 5428.
(48) Lehmann, V. *J. Electrochem. Soc.* **1996**, *143*, 1313.
(49) Sperling, J.; Jungblut, H.; Lewerenz, H. J. To be published.